Terr. Atmos. Ocean. Sci., Vol. 28, No. 5, 715-737, October 2017 doi: 10.3319/TAO.2017.01.06.01

Estimation of seismic ground motions and attendant potential human fatalities from scenario earthquakes on the Chishan fault in southern Taiwan

Kun-Sung Liu *

Department of Civil Engineering & Hazard Mitigation Research Center, Kao Yuan University, Kaohsiung City, Taiwan

Article history:
Received 19 August 2016
Revised 6 January 2017
Accepted 6 January 2017

Keywords:
Chishan Fault, Potential Human Fatality, Ground Motion, Shake Map, Southern Taiwan

Citation:
Liu, K.-S., 2017: Estimation of seismic ground motions and attendant potential human fatalities from scenario earthquakes on the Chishan fault in southern Taiwan. Terr. Atmos. Ocean. Sci., 28, 715-737, doi: 10.3319/TAO.2017.01.06.01

ABSTRACT

The purpose of this study is to estimate maximum ground motions in southern Taiwan as well as to assess potential human fatalities from scenario earthquakes on the Chishan active faults in this area. The resultant Shake Map patterns of maximum ground motion in a case of M_w 7.2 show the areas of PGA above 400 gals are located in the northeastern, central and northern parts of southwestern Kaohsiung as well as the southern part of central Tainan, as shown in the regions inside the yellow lines in the corresponding figure. Comparing cities with similar distances located in Tainan, Kaohsiung, and Pingtung to the Chishan fault, the cities in Tainan area have relatively greater PGA and PGV, due to large site response factors in Tainan area. Furthermore, seismic hazards in terms of PGA and PGV in the vicinity of the Chishan fault are not completely dominated by the Chishan fault. The main reason is that some areas located in the vicinity of the Chishan fault are marked with low site response amplification values from 0.55 - 1.1 and 0.67 - 1.22 for PGA and PGV, respectively. Finally, from estimation of potential human fatalities from scenario earthquakes on the Chishan active fault, it is noted that potential fatalities increase rapidly in people above age 45. Total fatalities reach a high peak in age groups of 55 - 64. Another to pay special attention is Kaohsiung City has more than 540 thousand households whose residences over 50 years old. In light of the results of this study, I urge both the municipal and central governments to take effective seismic hazard mitigation measures in the highly urbanized areas with a large number of old buildings in southern Taiwan.

1. INTRODUCTION

Recently, the M_L 6.6 Meinong earthquake on 6 February 2016 in southern Taiwan caused significant damage to nearby cities, especially with 115 people killed in the collapsed Weiguan Building. Historically, there were many damaging earthquakes in southern Taiwan during the last century. Some of these earthquakes had resulted in heavy loss of human lives. They occurred primarily at shallow depths, and were mostly associated with active faults that ruptured the ground surface. Accordingly, the assessment of potential seismic hazards has become increasingly important in southern Taiwan, including Kaohsiung, Tainan, and northern Pingtung areas since the Central Geological Survey upgraded the Chishan active fault from suspected fault to Category I in 2010 (CGS 2014). It poses a high potential for seismic disaster in the event of a large magnitude earthquake on the fault that most likely could cause serious damage. Hence, we need to put in more efforts on earthquake disaster prevention in these areas to reduce probably earthquake losses.

In addition, the Taiwan Earthquake Model (TEM) team, comprised of geologists, seismologists and engineering seismologists, assesses the probabilistic seismic hazards for Taiwan by considering potential social and economic impacts from various aspects of geology, seismology, and engineering. From the results of these studies, the highest hazard probability is evaluated to be in Southwestern Taiwan (Wang et al. 2016). Earthquakes have caused great loss of lives in Taiwan. Hence, National Science Council (NSC) of Taiwan started the HAZ-Taiwan project to promote research on seismic hazard analysis (Yeh et al. 2006).

* *Corresponding author*
E-mail: tf0143@cc.kyu.edu.tw

Reliable assessment of seismic hazards is a fundamental requirement for effective earthquake disaster mitigation. Reliable seismic hazard assessment, in turn, requires accurate ground motion estimates. In addition, some studies estimated potential seismic hazards in southern Taiwan in the form of Shake Maps. Particularly, the site response factor is incorporated into their ground motion prediction models to obtain more realistic peak ground motion estimates for assessment of potential seismic hazards (Liu et al. 2013a, b, 2014; Liu and Tsai 2015a).

The Shake Map developed by USGS provides a means of generating not only peak ground acceleration and velocity maps, but also a Modified Mercalli Intensity (MMI) map (Wald et al. 1999). This map makes it easier to relate the recorded ground motions to the shaking intensity and attendant damage. Recent Shake Map studies based upon maximum ground motion analyses showed areas of MMI intensity greater than VIII in the Chianan plains (Liu et al. 2013b). In addition, Liu and Tsai (2016a) applied a formula established by Tsai et al. (2001) that relates the human fatality rate with age, together with the age distribution of the population that could be affected by scenario earthquakes on Meishan, Chukou, and Hsinhua active faults in Chianan area to estimate the potential death tolls due to large future earthquakes.

In this study, I first estimate the maximum seismic ground motions in term of PGA, PGV, and MMI, aiming to show high seismic hazard areas in southern Taiwan. Furthermore, I will assess potential death tolls due to large future earthquakes occurring on the Chishan active fault. The results of this study will show areas with high earthquake disaster potential. They can serve as critical information for emergency response planning. They will also provide valuable information for site evaluation of critical facilities in high earthquake hazard regions.

2. THE STUDY AREA AND DATA USED

According to the active fault map of Taiwan published by the Central Geological Survey (CGS 2014), the Kaohsiung area has three active faults. One of them belongs to Type I, namely Holocene active fault, with its number and name as follows: 23 Chishan fault. Two active faults belong to Type II, namely late Pleistocene active faults as follows: 22 Hsiaokangshan fault, 24 Chaochou fault, respectively. In 2006, seismic micro zonation for considering the Type I active fault was implemented in the Building Seismic Design Code. Hence, I will focus on the Chishan active fault to estimate the maximum ground motions and attendant potential human fatalities in Southern Taiwan.

At first, the focal depth and length for the scenario earthquakes on Chishan fault were assumed to be 10 and 30 km, respectively, based on the information from Taiwan Earthquake Loss Estimation System (TELES) developed by the National Center for Research on Earthquake Engineering (NCREE) (Yeh et al. 2006) and CGS (2014). Another study to identify thirty-eight on-land active seismogenic structures by Shyu et al. (2016) also provided the general information for Chishan fault is southeast of Tainan, dips at 75°, and extends to a depth of 10.8 km. According the empirical relationships among magnitude and rupture length of fault developed by Wells and Coppersmith (1994). The reasonable magnitude value for Chishan fault would be M_w 6.8 and 7.2 corresponding to a fault length of 30 and 70 km, respectively. However, from the other Type I active faults in Taiwan, the empirical relationships conducted by Wells and Coppersmith (1994) are not completely suitable. For example, such as Tuntzuchiao fault and Shihtan fault with lengths of 14 and 12 km for M 7.1 earthquake (Construction and Planning Agency, Ministry of the Interior 2006; CGS 2014). Hence, considering the uncertainty and possibility, three magnitude values of M_w 6.8, 7.0, and 7.2, respectively, will use to estimate the maximum ground motions.

Our study area of southern Taiwan covers these jurisdictions of Tainan City, Kaohsiung City, and Pingtung County (Fig. 1). Tainan City area encompasses Chianan Plain and Foothills with landscapes sloping downward from east to west. High terrains are located in the east with a maximum elevation of 1233 m. Two-thirds of the whole Tainan region has elevation below 100 m, including ancient wetlands and lagoons with sandy soils (Council of Agriculture, Executive Yuan 2011). Between the Chiayi Hills and the west coast is the gently sloping Chianan Coastal Plain, the most important agricultural area in Taiwan. This basin is filled with Quaternary coastal and fluvial sediments up to 1500 - 2000 m thick (Shyu et al. 2005).

According to Shyu et al. (2005) and Sun et al. (2016), southern Taiwan which includes the cities of Tainan and Kaoshiung as well as Pingtung county, are located in the Kaoping structural domain which consists of shallow marine bedrock from the continental shelf that is being uplifted and deformed as part of crustal shortening during orogenic collision. The Kaoping Domain includes a rapidly subsiding basin, between the Central Range and the Western Foothills. On land, NE-SW striking right-lateral faults and N-S striking folds dominate the deformation of the Western Foothills. The Kaoping domain also includes the Pingtung plain between the Central Range and the Western Foothills, where Holocene subsidence is occurring at rates up to 13 mm yr^{-1} (Shyu et al. 2005). The Pingtung Plain is bounded by NE-SW trending left lateral oblique strike-slip faults. The Chishan fault lies along the western border of the Pingtung Plain. The Pingtung Valley in southern Taiwan is located between the lofty Central Range on the east and a low hilly upland on the west. The Central Range extends immediately southward, forming the Hengchun Peninsula east of the Pingtung Valley. The hilly upland on the west is the southern end of the western foothill zone. The Pingtung Valley is a sediment-filled

trough, having a north-south length of 55 km and an east-west width averaging 20 km. Pingtung is the main city on this plain (Ho 1982).

Tainan City has 37 jurisdiction districts with a total population of 1882777. Kaohsiung City has 38 jurisdiction districts with a total population of 2779355. Pingtung County, under its jurisdiction has 33 townships with a total population of 849734 (National Statistics 2014). The administrative districts of southern Taiwan are shown in Figs. 1 and 2, respectively. The distribution of average

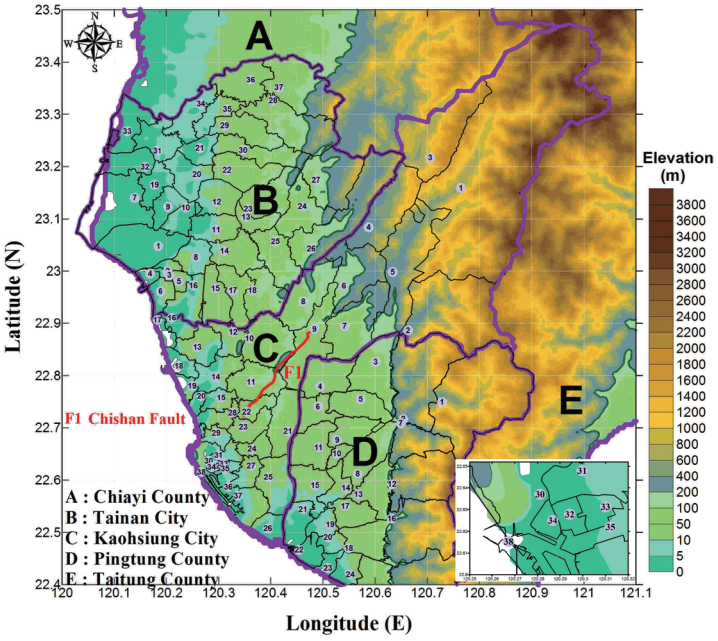

Fig. 1. Topographic map of the southern Taiwan, showing the Type I Chishan active fault and 37, 38, and 24 administrative districts in Tainan City, Kaohsiung City, and northern Pingtung County, respectively. The corresponding names of the administrative districts are given in Table 1. (Inset) Location of administrative districts in southwest Kaohsiung City.

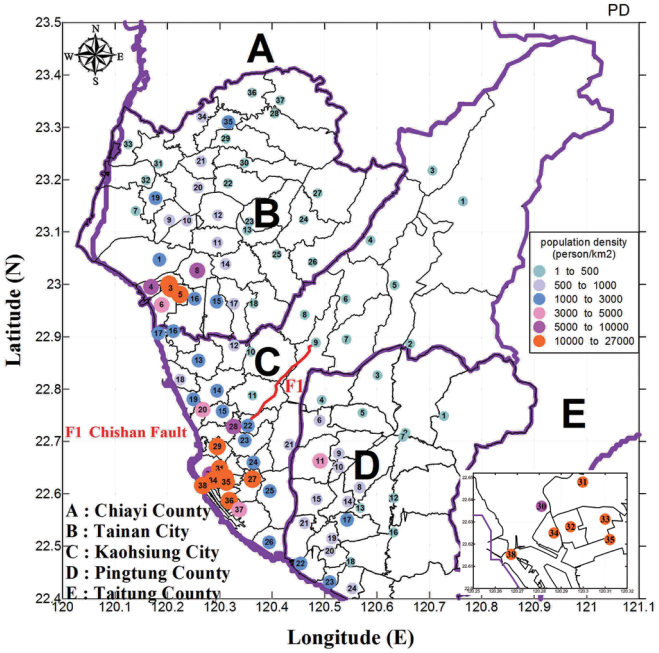

Fig. 2. Population density map of southern Taiwan. The Type I Chishan active fault and 37, 38, and 24 administrative districts in Tainan City, Kaohsiung City, and northern Pingtung County, respectively, are also shown. The corresponding names of the administrative districts are given in Table 1. (Inset) Location of administrative districts in southwest Kaohsiung City.

population density in the area is also shown in Fig. 2 and given in Table 1 (National Statistics 2014). Areas of high population density between 5000 and 10000 per km^2 can be seen in Anping and Yongkang districts of Tainan City as well as Nanzih and Gushan districts of Kaohsiung City. Furthermore, areas of high population density above 10000 per km^2 can be seen in North, West Central, and East districts of Tainan City as well as Fongshan, Zuoying, Sanmin, Cianjin, Sinsing, Yancheng, Lingya, Cianjhen, and Cijin districts of Kaohsiung City. Compounded with rapid

Table 1. Population and Population density of the administrative districts of southern Taiwan.

Tainan City (1882777)				Kaohsiung City (2779355)				Pingtung County (849734)			
No	**Region**	**Pop.**	**Pop.D.**	**No**	**Region**	**Pop.**	**Pop.D.**	**No**	**Region**	**Pop.**	**Pop.D**
1	Annan	187775	1752	1	Taoyuan	4296	5	1	Wutai	3435	12
2	North Dist.	132558	12704	2	Maolin	1915	10	2	Sandimen	7784	40
3	West Central	77910	12446	3	Namasia	3204	13	3	Gaoshu	25520	283
4	Anping	64898	5864	4	Jiasian	6420	52	4	Ligang	26814	389
5	East Dist.	190233	14180	5	Liouguei	13663	70	5	Yanpu	26629	414
6	South Dist.	125691	4609	6	Shanlin	12531	120	6	Jiouru	22172	528
7	Cigu	23608	214	7	Meinong	41258	344	7	Majia	6718	85
8	Yongkang	228651	5677	8	Neimen	15178	159	8	Neipu	56148	686
9	Sigang	24896	737	9	Cishan	38100	403	9	Changjhih	30429	763
10	Anding	30298	969	10	Tianliao	7680	83	10	Linluo	11313	696
11	Sinshih	35482	742	11	Yanchao	30397	465	11	Pingtung	203866	3133
12	Shanhua	46100	833	12	Alian	29566	854	12	Taiwu	5289	45
13	Shanshang	7500	269	13	Lujhu	53064	1096	13	Wanluan	20918	344
14	Sinhua	43782	706	14	Gangshan	97751	2039	14	Jhutian	17719	609
15	Gueiren	67504	1210	15	Ciaotou	37198	1434	15	Wandan	52085	906
16	Rende	73099	1440	16	Hunei	29399	1458	16	Laiyi	7648	46
17	Guanmiao	34865	650	17	Jiading	30690	1947	17	Chaojhou	54738	1290
18	Longci	4292	67	18	Yongan	14148	626	18	Sinpi	10232	173
19	Jiali	59533	1529	19	Mituo	19854	1344	19	Kanding	16374	524
20	Madou	45067	835	20	Zihguan	36384	3137	20	Nanjhou	11026	581
21	Siaying	25068	748	21	Dashu	43190	645	21	Sinyuan	36692	958
22	Guantian	21706	307	22	Dashe	34455	1296	22	Donggang	48262	1638
23	Danei	10248	146	23	Renwu	80994	2245	23	Linbian	19235	1231
24	Yujing	14561	191	24	Niaosong	43735	1778	24	Jiadong	20247	653
25	Zuojhen	5181	69	25	Daliao	111191	1565	25	Chunrih	4866	30
26	Nanhua	9001	52	26	Linyuan	70476	2183	26	Fangliao	25482	441
27	Nansi	10116	92	27	Fongshan	354093	13233	27	Shihzih	4882	16
28	Dongshan	21920	175	28	Nanzih	178532	6912	28	Fangshan	5749	333
29	Liouying	21828	356	29	Zuoying	195643	10094	29	Mudan	4864	27
30	Lioujia	22832	338	30	Gushan	135667	9196	30	Manjhou	8126	57
31	Syuejia	26949	499	31	Sanmin	347619	17568	31	Checheng	9121	183
32	Jiangjyun	20568	490	32	Cianjin	27832	14985	32	Hengchun	30859	226
33	Beimen	11691	265	33	Sinsing	52534	26581	33	Liouciou	12675	1863
34	Yanshuei	26322	504	34	Yancheng	25400	17937				
35	Sinying	78231	2030	35	Lingya	175854	21571				
36	Houbi	24589	340	36	Cianjhen	193952	10144				
37	Baihe	29731	235	37	Siaogang	156171	3790				
				38	Cijin	28958	19781				

urban growth and development, population increase, and the slow rebuilding of old buildings, any major earthquake is likely to cause severe damages. Effective earthquake disaster prevention measures in the region will be critical in order to reduce future earthquake loss (Liu and Tsai 2014, 2015b, 2016b).

3. METHODOLOGY

3.1 Maximum Ground Motion Parameters

At present, ground motions, in terms of either PGA or PGV, are estimated using the respective empirical attenuation relationship, which is a predictive relationship that allows estimation of peak ground motions at a given distance for an assumed earthquake magnitude. To obtain Shake Map, I use the relationship provided by Liu and Tsai (2005) for conversion from peak acceleration and velocity. In addition, a Modified Mercalli Intensity (MMI) map also has uses in combination by PGA and PGV. This MMI map makes it easier to relate the recorded ground motions to the shaking intensity and attendant damage.

Because quantitative site description of Vs30, the average shear-wave velocity over the top 30 m, is not available for all strong-motion sites of CWB (Liu et al. 1999), the conventional attenuation analysis cannot include a site response factor in the ground motion attenuation relationship of Liu and Tsai (2005). Alternatively, the site effect was corrected in this study by a site response factor at each grid point. I first use these predictive relationships to estimate peak ground motion for each grid point, and then corrects the amplitude at that location using a site response factor determined by Liu and Tsai (2005, 2015a).

The following equation form is used in this study (Liu and Tsai 2005):

$$\ln(\mathrm{PGA, PGV}) = a\ln\left[X + h_1 \exp^{(h_2 M_W)}\right] + bX + cM_W + d \quad (1)$$

where PGA and PGV are ground motion parameters, X is the closest distance to the rupture surface, M_w is moment magnitude, a is geometrical spreading coefficient, b is an elastic attenuation coefficient, c is magnitude coefficient, d is a constant, h_1 and h_2 are close-in distance saturation coefficient. The coefficients a, b, c, d, h_1, and h_2 are to be determined by regression from the data.

In addition, the residual value, i.e., site response factor, is defined as the difference between the logarithms of the observed and the predicted ground motion, and is expressed by the following equation:

$$r = \ln Y_S - \ln Y_r = \eta + \varepsilon \quad (2)$$

Where Y_S is the observed value, Y_r is the predicted value of the Eq. (1), η is the earthquake inter-event errors with standard deviation equal to τ, and ε is intra-event errors with standard deviation equal to σ. The η and ε are assumed to be independent normally distributed variants with variances τ^2 and σ^2. The standard deviation of total residual σ_T is given by the equation

$$\sigma_T = \sqrt{\sigma^2 + \tau^2} \quad (3)$$

The residuals due to regression were decomposed into inter-event (earthquake-to-earthquake) and intra-event residuals. The inter-event and intra-event residuals are calculated by the Eqs. (3.15) and (3.16) in Campbell and Bozorgnia (2007).

In this study, I denote the total residual (r) as the site response factor and the intra-event residual (ε) as the site effect factor, respectively. The site response factor includes both source and site effects relative to the recording station, whereas the site effect factor only includes site effect. The site response amplification values and site effect amplification values can be calculated from exp(r) and exp(ε), respectively. The site total and intra-event residuals for the TSMIP stations are referred in Liu and Tsai (2015a).

The corresponding contour maps of total residuals of 627 stations for the horizontal PGA and PGV, respectively in southern Taiwan are shown in the Figs. 3 and 4. A total of 627 stations of the Taiwan Strong Motion Instrumentation Program (TSMIP) and Central Mountain Strong Motion Array (CMSMA) networks are used to generate the site response factor map with a block size of 0.01° × 0.01° (or roughly 1 km × 1 km) (Liu and Tsai 2015a). The maps with small grid size were interpolated based on the 627 stations for the calculations of hazard maps and human fatalities. These free-field stations are densely spaced approximately 5 km apart, especially only about 3 km in urban areas (Liu et al. 1999). In addition, the site amplification values of intra-event residuals relative to a NEHRP B/C boundary site condition (Vs30 = 760 m s^{-1}) for PGA and PGV, respectively are plotted in Figs. 5 and 6. These two figures are extracted from the Figs. 6 and 7 of Liu and Tsai (2015a).

In brief, I devise a two-dimensional surface grid map with a block size of 0.01° × 0.01° (or roughly 1 km × 1 km) across the entire study area. This is followed by a procedure to construct the Shake Maps, as follows: first, I use the empirical attenuation relationships obtained from Taiwan by Liu and Tsai (2005) to calculate PGA and PGV for earthquakes in the database at each grid point. In this step, the active fault of Type I, Chishan fault was used as a line source to calculate the maximum ground motion. Second, a site response factor is used to correct above PGA and PGV at all grid points, as shown in Figs. 3 and 4. Finally, I combine above results with the estimated PGA and PGV into MMI maps. The maximum ground motion parameters

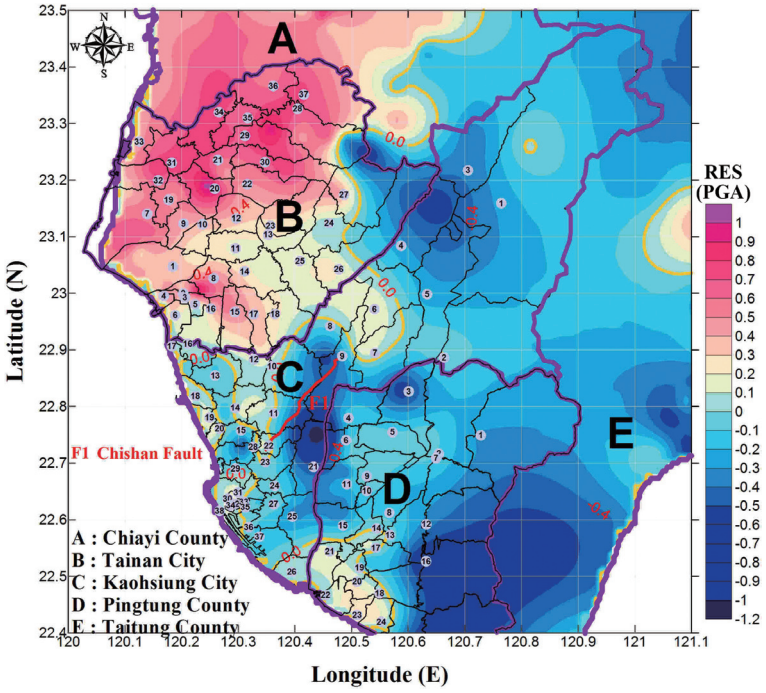

Fig. 3. Distribution of the site response factor for PGA in southern Taiwan. The site response factor is defined as the residual value r, that is the difference between logarithms for the observed and predicted PGA. The site response amplification values can be calculated from exp(*r*).

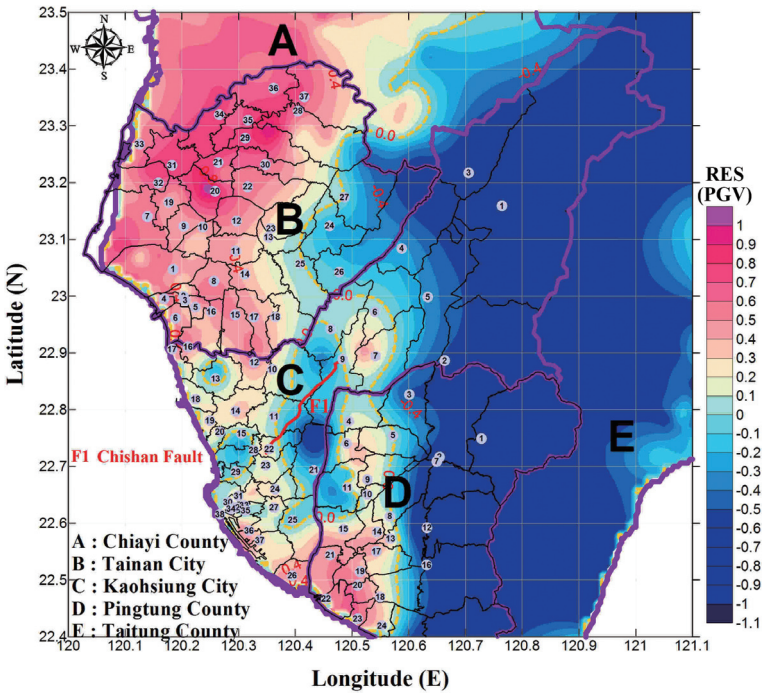

Fig. 4. Distribution of the site response factor for PGV in southern Taiwan. The site response factor is defined as the residual value *r*, that is the difference between logarithms for the observed and predicted PGV. The site response amplification values can be calculated from exp(*r*).

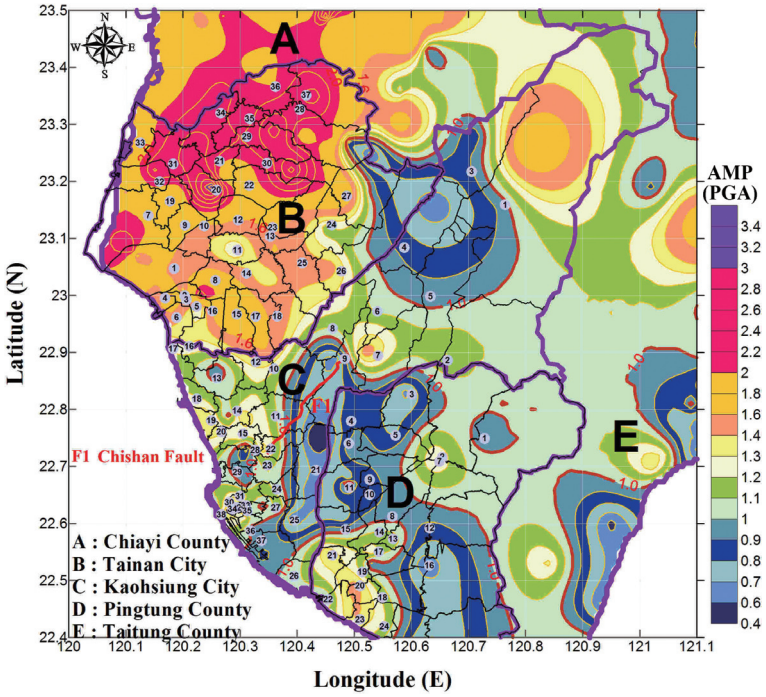

Fig. 5. Distribution of the site amplification values for intra-event residuals relative to a NEHRP B/C boundary site condition (Vs30 = 760 m s^{-1}) for PGA.

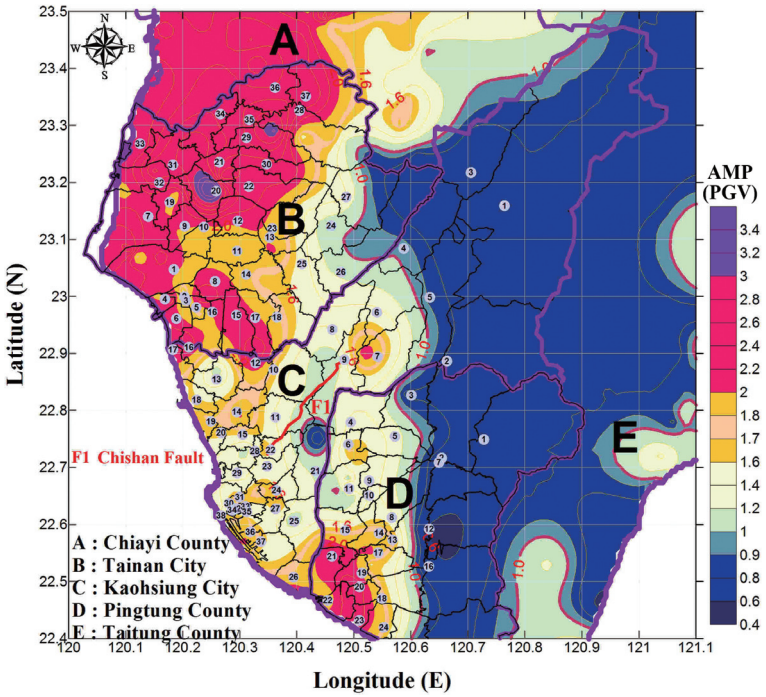

Fig. 6. Distribution of the site amplification values for intra-event residuals relative to a NEHRP B/C boundary site condition (Vs30 = 760 m s^{-1}) for PGV.

inside a block provide a means to assess the potential earthquake hazard in a region.

In this study, ground shaking selected both for the Modified Mercalli Intensity (MMI) scale and the Taiwan intensity scale used by the Central Weather Bureau (CWB) of Taiwan is given in Tables 2 (http://earthquake.usgs.gov/eqcenter/shakemap/background.php) and 3 (http://www.cwb.gov.tw/in/seismic/quake_preparedness.htm), respectively. On the MMI intensity scale, the levels of earthquake shaking are designated as light damage (MMI VI), moderate damage (MMI VII), and heavy damage (MMI VIII). Likewise, on the CWB intensity scale (CWBI), the levels of earthquake shaking are designated as minor damage (CWBI V), moderate damage (CWBI VI), and severe damage (CWBI VII).

3.2 Assessment of Human Fatality

To be effective an earthquake protection program needs to include realistic estimation of life loss in future earthquakes. Yet empirical data that document the occurrences of fatalities in earthquakes are relatively rare (Coburn and Spence 1992; Tsai et al. 2001). Tsai et al. (2001) made a realistic assessment of probable levels of human casualties caused by the 1999 Chi-Chi earthquake in Taiwan. The results showed clear age dependence of the human-fatality rate based on demographic data of the two hardest-hit Nantou and Taichung counties. Accordingly, a realistic estimation of total human fatalities in areas of high seismic intensity, either before a large earthquake by performing scenario studies, or shortly after a real earthquake by a system of rapid intensity mapping can be made. The age dependence of human fatality rate used in this study to calculate the number of fatalities is expressed as follows (Tsai et al. 2001; Yu 2004):

$$Y\% = 0.00022X^2 - 0.01X + 0.16 \quad (4)$$

where $Y\%$ is the age-group fatality rate in percentage, and X represents age.

The above equation was conducted by Yu (2004) according the total fatalities in individual townships located inside the seismic intensity greater than 250 gals in Nantou and Taichung counties. Because the Chi-Chi earthquake struck late at night (1:47 AM, local time), almost all residents were at home. In fact, most people in the strongly shaken rural areas were in bed. As a result, building collapse became the most dominant cause of fatalities (Tsai et al. 2001). Hence, the fatality rate model in this study should be more suitable for night time. On the other hand, the primary cause of death of the victims of the Chi-Chi earthquake was structural failure and the building types was cited as one of the most important factors affected this (Pai et al. 2007). Due to building code revisions after 1999, better building quality is expected and corresponding fatality rate should be reduced.

4. RESULTS AND DISCUSSION

4.1 Maximum Ground Motion Parameters

The studies of ground motion characteristics in Taiwan require ground-motion attenuation models. Attenuation

Table 2. Modified Mercalli Intensity Scale (MMI).

Estimated Intensity		I	II-III	IV	V	VI	VII	VIII	IX	X+
Peak Acc.	%g	< 0.17	0.17 - 1.4	1.4 - 3.9	3.9 - 9.2	9.2 - 18	18 - 34	34 - 65	65 - 124	> 124
	gal	< 1.7	1.7 - 13.7	13.7 - 38.2	38.2 - 90.2	90.2 - 176	176 - 333	333 - 637	637 - 1215	> 1215
Peak Vel.(cm s^{-1})		< 0.1	0.1- 1.1	1.1 - 3.4	3.4 - 8.1	8.1 - 16	16 - 31	31 - 60	60 - 116	> 116
Perceived Shaking		Not Felt	Weak	Light	Moderate	Strong	Very Strong	Severe	Violent	Extreme
Potential Damage		None	None	None	Very Light	Light	Moderate	Moderate/Heavy	Heavy	Very Heavy

Table 3. Central Weather Bureau Intensity Scale (CWBI) of Taiwan.

Intensity Scale	0	1	2	3	4	5	6	7
	Micro	Very minor	Minor	Light	Moderate	Strong	Very Strong	Great
Peak Acc. (cm s^{-2})	< 0.8	0.8 - 2.5	2.5 - 8.0	8 - 25	25 - 80	80 - 250	250 - 400	> 400
Effects Or Damage			Hanging lamps vibrate slightly.	Buildings shake, hanging objects shake visibly.	Buildings rock noticeably; may cause slight damage.	Walls crack; some chimneys and large archways topple over.	Damage to some buildings, doors and windows bend.	Severe damage to or collapse of some buildings; underground lines break.

relationships, or "Ground Motion Prediction Equations (GMPEs)", provides an efficient means for predicting the level of ground shaking and its associated uncertainty at any given site or location, as well as for use in seismic hazard analyses (Bolt and Abrahamson 2003). The value of the maximum ground motion parameters is calculated at each grid point of the study area to contour the Shake Map. As explained earlier, I use three magnitude values of M_w 7.2, 7.0, and 6.8, respectively, for Cases 1 - 3 to estimate the maximum ground motions.

4.1.1 Case 1 for M_w 7.2

Figure 7 shows the maximum PGA Shake Map for an M_w 7.2 scenario earthquake on the Chishan active fault in southern Taiwan. Locations of the 37 administrative districts of Tainan City, 38 administrative districts of Kaohsiung City and 24 administrative districts of Northern Pingtung as well as Chechen fault are also shown. The results reveal that high PGA areas greater than 400 gals, corresponding to CWB intensity greater than VII, are located in the following regions: southwestern Shanlin, northwestern Meinong, Neimen, northern Cishan, central and western Tianliao, central and western Yanchao, Alian, eastern Gangshan, Ciaotou, eastern Mituo, Zihguan, central and western Dashe, central and western Renwu, western Niaosong, northern Fongshan, Nanzih, Zuoying, eastern Gushan, Sanmin, Cianjin, northern Sinsing, and Yancheng in the Kaohsiung City. Similarly, high PGA areas greater than 400 gals are also located in eastern North Dist., northern East Dist., southern Yongkang, eastern Gueiren, central and southern Guanmiao, central and southern Longci, southern Zuojhen, and southern Nanhua in the Tainan City. Likewise, I obtain the maximum PGV Shake Map as shown in Fig. 8. It can be seen that the areal patterns of high PGV greater than 50 cm s^{-1}, corresponding to MMI intensity greater than VIII, are similar to that of the PGA.

Seismic intensity, especially for that of the MMI is widely used to represent the level of ground shaking following a damaging earthquake (Wald et al. 1999). Hence, I obtain an MMI intensity map, based on a combination of estimated maximum PGA and PGV, as shown in Fig. 9. It can be seen that the patterns of high MMI greater than VIII, are similar to the contour pattern of the PGV greater than 31 cm s^{-1}. In summary, the Shape Maps shown in Figs. 7 - 9 can provide critical information to assess potential earthquake hazards in southern Taiwan.

4.1.2 Case 2 for M_w 7.0

Figure 10 shows the maximum PGA Shake Map for an M_w 7.0 scenario earthquake on the Chishan active fault in southern Taiwan. Locations of the 37 administrative districts of Tainan City, 38 administrative districts of Kaohsiung City and 24 administrative districts of Northern Pingtung as well as the Chechen fault are also shown. The results reveal that high PGA areas greater than 400 gals, corresponding to CWB intensity greater than VII, are located in the following regions: southwestern Shanlin, northwestern Meinong, eastern Neimen, northeastern Cishan, southwestern Tianliao, western Yanchao, eastern Gangshan, northeastern Ciaotou, western Dashe, western Renwu, northeastern Nanzih, and southeastern Zuoying in the Kaohsiung City. In addition, high PGA areas greater than 400 gals are also located in southern Guanmiao in the Tainan City. Likewise, I obtain the maximum PGV Shake Map as shown in Fig. 11. It can be seen that the areal patterns of high PGV greater than 50 cm s^{-1}, corresponding to MMI intensity greater than VIII, are similar to that of the PGA.

Next, I obtain an MMI intensity map, based on a combination of estimated maximum PGA and PGV, as shown in Fig. 12. It can be seen that the patterns of high MMI greater than VIII, are similar to the contour pattern of the PGV greater than 31 cm s^{-1}.

4.1.3 Case 3 for M_w 6.8

Figure 13 shows the maximum PGA Shake Map for an M_w 6.8 scenario earthquake on the Chishan active fault in southern Taiwan. Locations of the 37 administrative districts of Tainan City, 38 administrative districts of Kaohsiung City and 24 administrative districts of Northern Pingtung as well as Chechen fault are also shown. The results reveal that high PGA areas greater than 400 gals, corresponding to CWB intensity greater than VII, are located in the following regions: northwestern Meinong and western Dashe in the Kaohsiung City. Likewise, I obtain the maximum PGV Shake Map as shown in Fig. 14. It can be seen that the areal patterns of high PGV greater than 40 cm s^{-1}, corresponding to MMI intensity greater than VIII, are similar to that of the PGA. Next, I obtain an MMI intensity map, based on a combination of estimated maximum PGA and PGV, as shown in Fig. 15. It can also be seen that the patterns of high MMI greater than VIII, are similar to that contour pattern of the PGV greater than 31 cm s^{-1}.

From Figs. 2 - 15 mentioned above, I can find the following features: (1) the higher magnitude for a scenario earthquake on the Chishan fault, the more land coverage and population affected in areas with PGA greater than 250 gals, corresponding to CWB intensity VI. For example, the population in areas affected PGA greater than 250 gals in Kaohsiung City from M_w 7.2, 7.0, 6.8 earthquakes are 2543359, 2074567, and 1349315, respectively. (2) The cities located in Tainan City at similar distances from the Chishan fault have comparatively larger PGA and PGV than those in Kaohsiung City and Pingtung County. Such a pattern is due to the effects of large site response factors. For example, the site response amplification values of 2.89 and 2.97 for PGA and PGV, respectively, can be found in Madou from

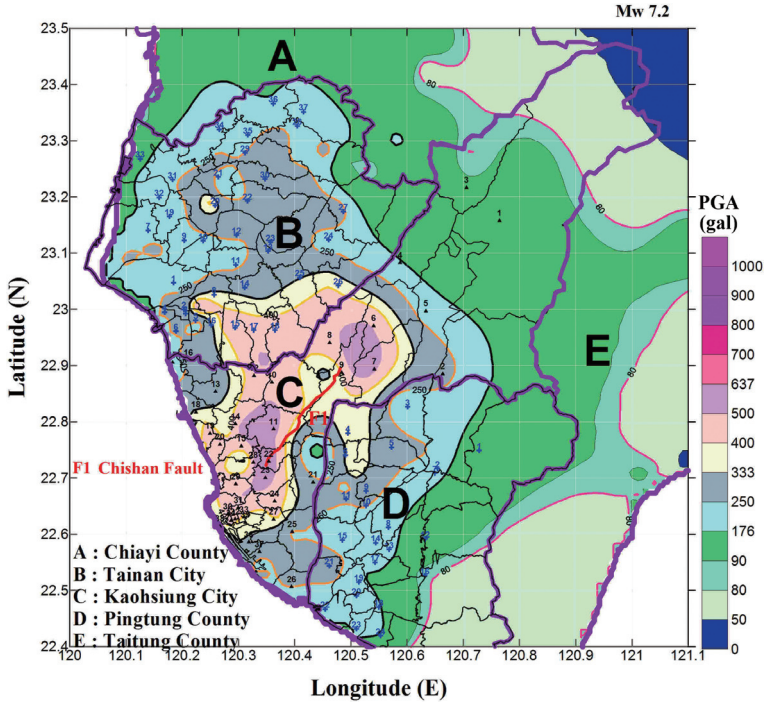

Fig. 7. The maximum PGA Shake Map for M_w 7.2 scenario earthquake on the Chishan active fault in southern Taiwan. Locations of the 37 administrative districts of Tainan City, 38 administrative districts of Kaohsiung City and 24 administrative districts of Northern Pingtung as well as Chishan fault are also shown.

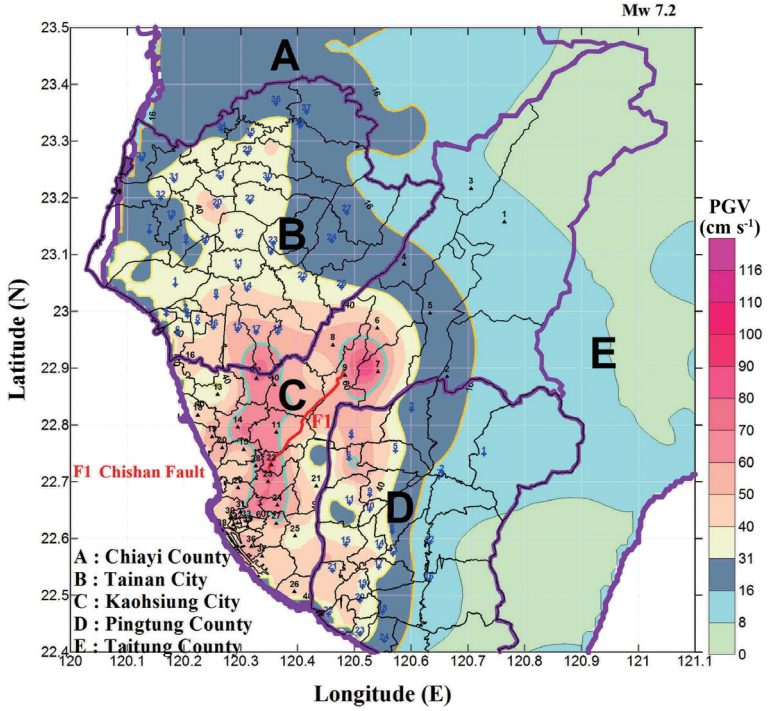

Fig. 8. The maximum PGV Shake Map for M_w 7.2 scenario earthquake on the Chishan active fault in southern Taiwan. Locations of the 37 administrative districts of Tainan City, 38 administrative districts of Kaohsiung City and 24 administrative districts of Northern Pingtung as well as Chishan fault are also shown.

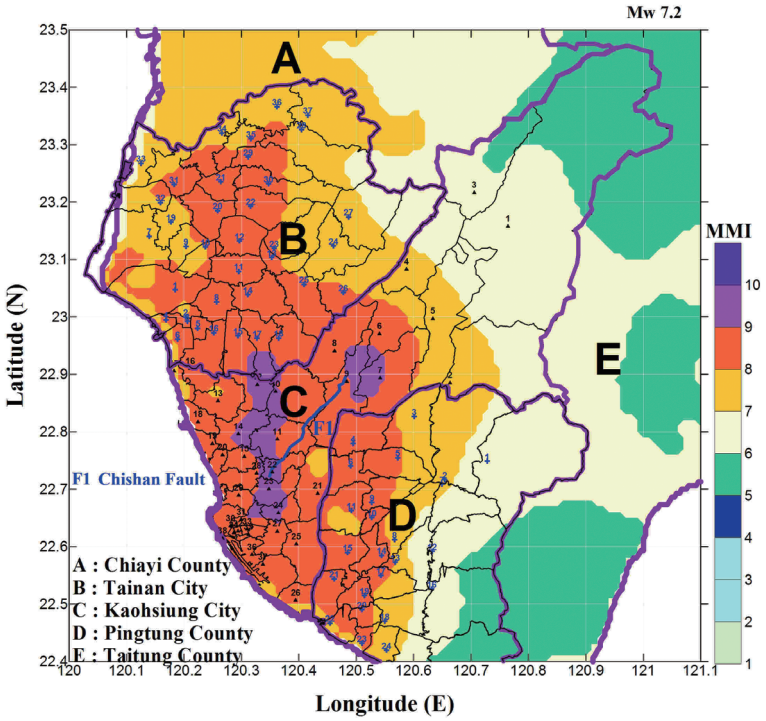

Fig. 9. The maximum MMI Shake Map for M_w 7.2 scenario earthquake on the Chishan active fault in southern Taiwan. Locations of the 37 administrative districts of Tainan City, 38 administrative districts of Kaohsiung City and 24 administrative districts of Northern Pingtung as well as Chishan fault are also shown.

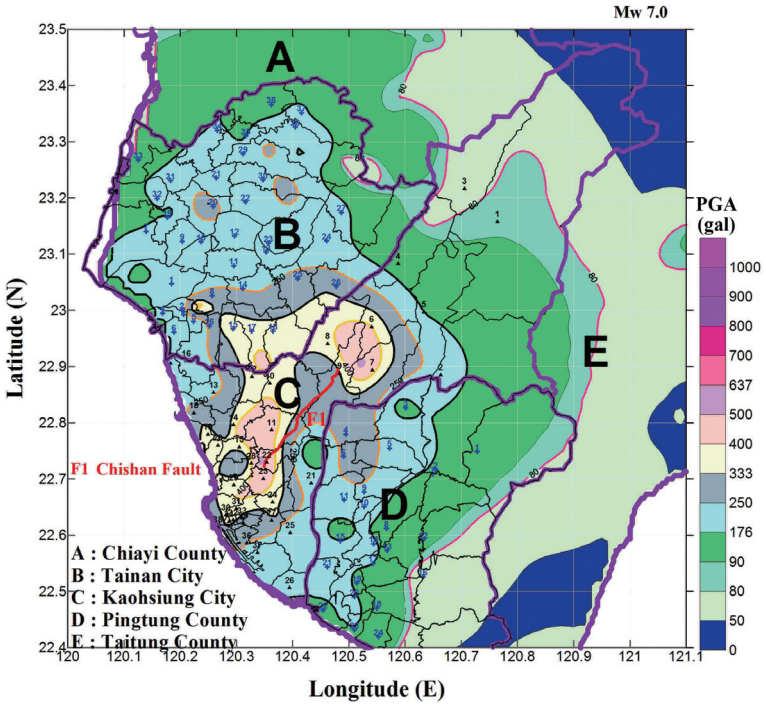

Fig. 10. The maximum PGA Shake Map for M_w 7.0 scenario earthquake on the Chishan active fault in southern Taiwan. Locations of the 37 administrative districts of Tainan City, 38 administrative districts of Kaohsiung City and 24 administrative districts of Northern Pingtung as well as Chishan fault are also shown.

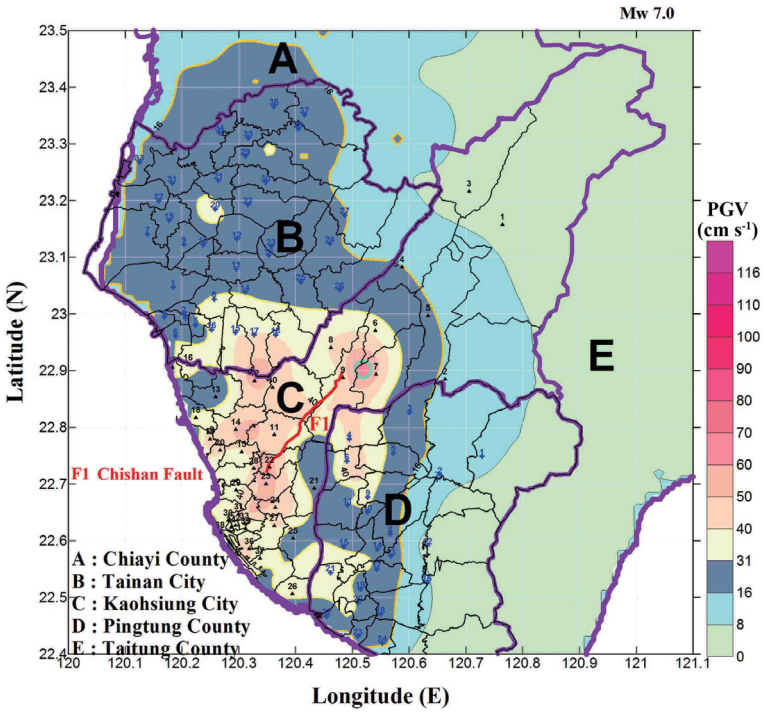

Fig. 11. The maximum PGV Shake Map for M_w 7.0 scenario earthquake on the Chishan active fault in southern Taiwan. Locations of the 37 administrative districts of Tainan City, 38 administrative districts of Kaohsiung City and 24 administrative districts of Northern Pingtung as well as Chishan fault are also shown.

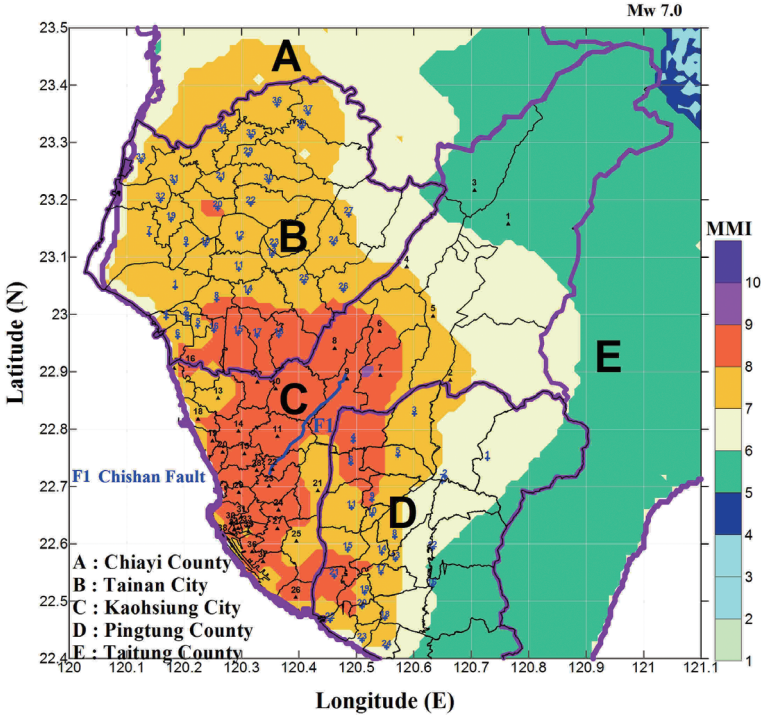

Fig. 12. The maximum MMI Shake Map for M_w 7.0 scenario earthquake on the Chishan active fault in southern Taiwan. Locations of the 37 administrative districts of Tainan City, 38 administrative districts of Kaohsiung City and 24 administrative districts of Northern Pingtung as well as Chishan fault are also shown.

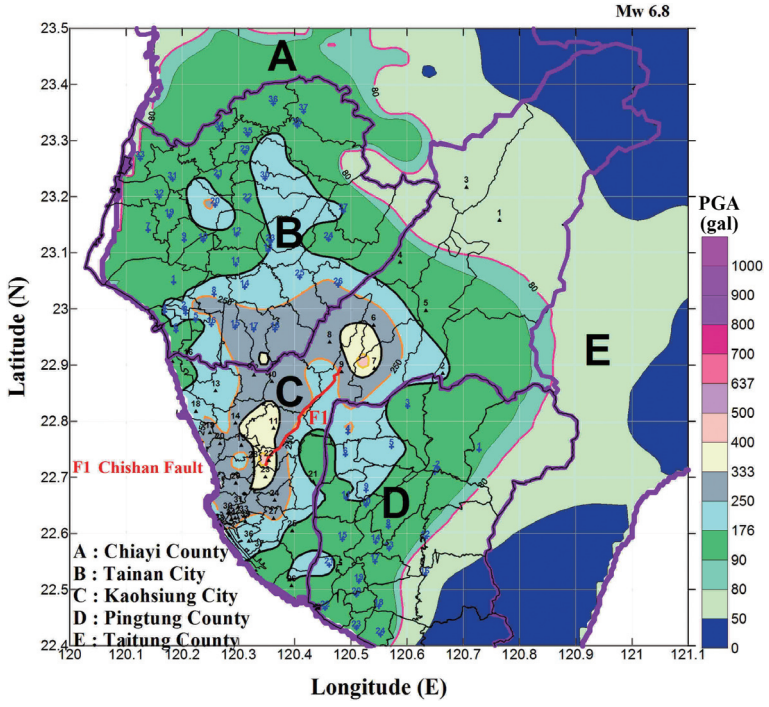

Fig. 13. The maximum PGA Shake Map for M_w 6.8 scenario earthquake on the Chishan active fault in southern Taiwan. Locations of the 37 administrative districts of Tainan City, 38 administrative districts of Kaohsiung City and 24 administrative districts of Northern Pingtung as well as Chishan fault are also shown.

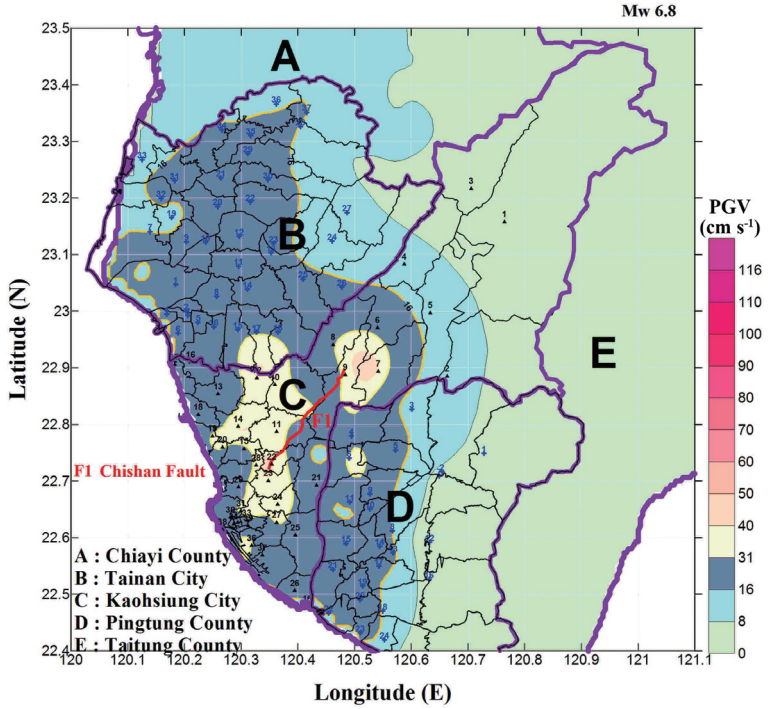

Fig. 14. The maximum PGV Shake Map for M_w 6.8 scenario earthquake on the Chishan active fault in southern Taiwan. Locations of the 37 administrative districts of Tainan City, 38 administrative districts of Kaohsiung City and 24 administrative districts of Northern Pingtung as well as Chishan fault are also shown.

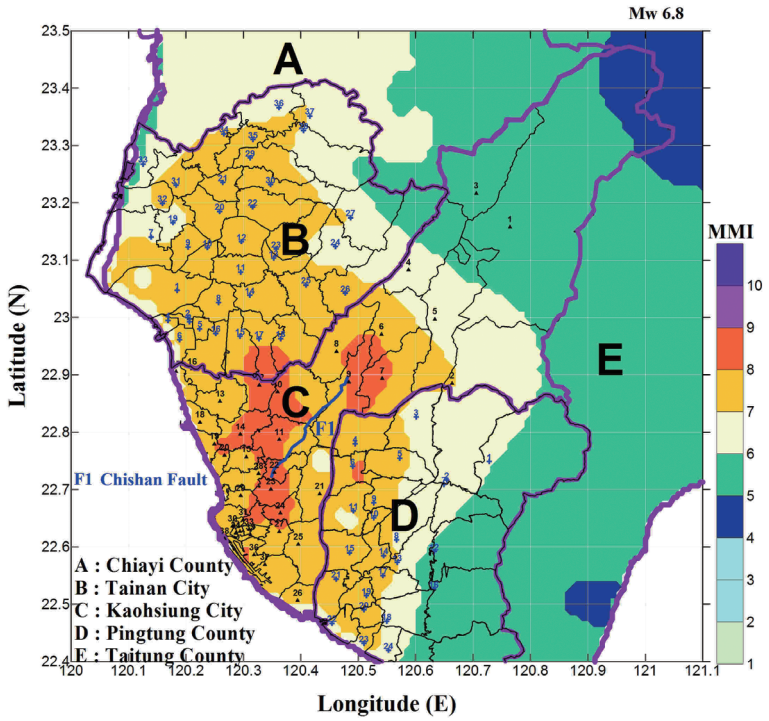

Fig. 15. The maximum MMI Shake Map for M_w 6.8 scenario earthquake on the Chishan active fault in southern Taiwan. Locations of the 37 administrative districts of Tainan City, 38 administrative districts of Kaohsiung City and 24 administrative districts of Northern Pingtung as well as Chishan fault are also shown.

Figs. 3 and 4. High site response amplification values ranging from 1.0 - 2.7 for both PGA and PGV are present in the western Tainan area as can also be found. On the other hand, seismic hazard in term of PGA and PGV respectively in Figs. 7 and 8 shown in the vicinity of the Chishan fault is not entirely dominated by the fault. The main reason is that the areas located in the vicinity of the Chishan fault are relative to the low site response factors as shown in Figs. 3 and 4. It can be found low site response amplification values [exp(r)] ranging from 0.55 - 1.1 and 0.67 - 1.22 for PGA and PGV, respectively, are present near the Chishan fault areas. It can also be found low site effect amplification values [exp(ε)] relative to a NEHRP B/C boundary site condition (Vs30 = 760 m s^{-1}) ranging from 0.6 - 1.2 and 1.0 - 1.6 for PGA and PGV, respectively, are present near the Chishan fault areas in Figs. 5 and 6. In other word, The PGA not always the highest values along the fault rupture area. The observed PGA contour pattern from Liu et al. (2013a) showed the PGA ranged from 300 - 900 gals along the rupture trace of the Chelungpu fault. Furthermore, the PGA of 324 gals recorded at TCU075 seismic station just with a distance of 0.3 km to the rupture trace of the Chelungpu fault (Chen et al. 2000). In addition, from a study of human-fatality in near-fault regions of the Chi-Chi earthquake (Pai et al. 2007), it was noted that, there were only 65 victims (2.6% of the total 2492 victims) inside the 15-m fault zone. These studies also showed that the site amplification factor plays an important role in seismic hazard assessment results (Liu and Tsai 2015b). (3) Seismic intensity, especially the MMI, is widely used to represent the level of ground shaking following a damaging earthquake (Wald et al. 1999). Hence, I obtained an MMI intensity map based on a combination of the estimated maximum PGA and PGV, as shown in Fig. 9. It can be seen that the patterns of high MMI greater than VIII, are similar to that of the PGV. In summary, the Shape Maps shown in Figs. 7 - 15 can provide critical information to assess potential earthquake hazards in southern Taiwan.

4.2 Potential Human Fatality Estimation from Earthquake Scenarios

Potential human fatality estimates were performed using the empirical function for human fatality rate age dependence for large earthquake scenarios in southern Taiwan obtained by Tsai et al. (2001). Three earthquake scenarios with M_w 7.2, 7.0, and 6.8 on the Chishan fault were used for this purpose.

In Case 1, a ground motion PGA Shake Map was calculated for an M_w 7.2 earthquake on the Chishan active fault using the empirical attenuation relationships by Liu and Tsai (2005), incorporating the site response factor in the predictive model, as shown in Fig. 7. Next, the age dependent fatality rate in Eq. (4) was combined with the impacted population data from the demographic summary

(National Statistics 2014) to calculate the number of potential fatalities, as shown in Figs. 16 - 18 for Kaohsiung City, Tainan City and Pingtung County, respectively.

The top panels in Fig. 16 show the fatality rates for individual age groups. The middle panels in Fig. 16 and the top panels of Figs. 17 - 18 show the age distributions for a total population of 2543359, 2074567, and 1349315 in the towns with estimated seismic intensity PGA greater than 250 gals in Kaohsiung City, Tainan City and Pingtung County, respectively as shown in Fig. 7. These figures indicate that the population numbers start to decrease steadily above age 55. Finally, the bottom panels in Figs. 16 - 18 and Table 4 show the age distributions for 5230, 2513, and 527 fatalities in Kaohsiung City, Tainan City and Pingtung County, respectively. For Kaohsiung City, as shown in Fig. 16c, the numbers of fatalities stay flat at an average of 103 for people below age 35. The fatalities then increase rapidly for those above age 45 and reach a high peak of 660 in the 60 - 64 age groups. The number of fatalities then drops rapidly back to 306 for those above age 85. For Tainan City, as shown in Fig. 17b, the numbers of fatalities stay flat at an average of 53 for people below age 35. The fatalities then increase rapidly for those above age 45 and reach a high peak of 280 in the 60 - 64 age groups. The number of fatalities then drops rapidly back to 156 for those above age 85. In Pingtung County, as shown in Fig. 18b, the numbers of fatalities stay flat at an average of 12 for people below age 35. The fatalities then increase rapidly for those above age 45 and reach a high peak of 59 in the 55 - 64 age groups. The number of fatalities then drops rapidly back to 36 for those above age 85.

For Cases 2 and 3, the ground motion PGA Shake Map calculated for M_w 7.0 and 6.8 earthquakes on the Chishan active fault respectively, are shown in Figs. 10 and 13. The corresponding numbers of fatalities in Kaohsiung City, Tainan City and Pingtung County, respectively are shown in Figs. 19 - 21 for M_w 7.0 and in Figs. 22 - 24 for M_w 6.8. The top panels in Figs. 19 - 21 show the age distributions

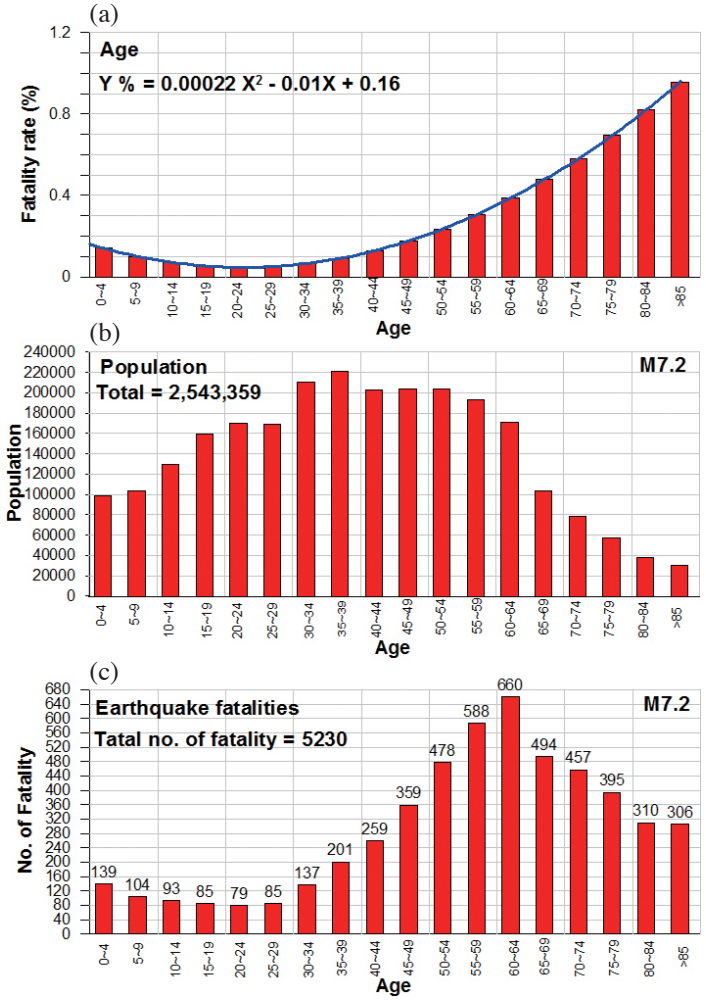

Fig. 16. Earthquake fatality rates (a), population (b), and the number of fatality (c) in Kaohsiung City estimated for an M_w 7.2 scenario earthquake on the Chishan active fault. A regression equation and corresponding curve on age dependence of the fatality rate is also shown in the top plot. (Color online only)

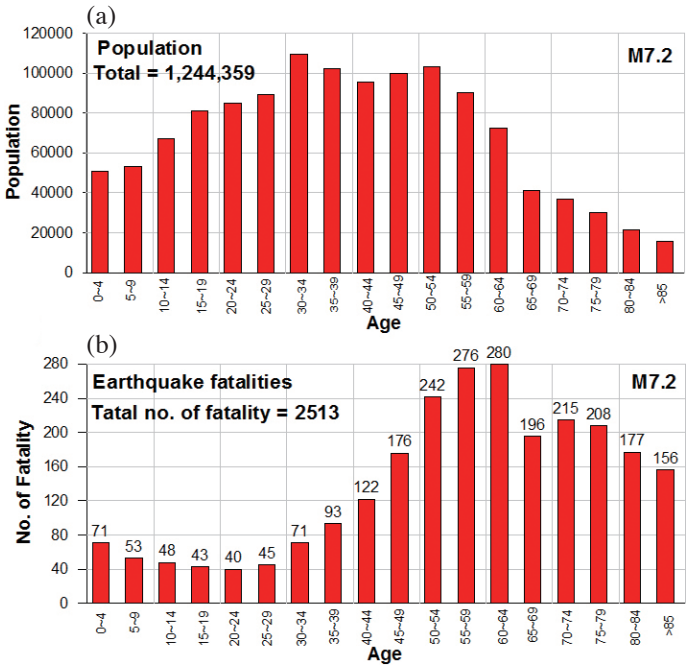

Fig. 17. Population (a) and the number of fatalities (b) in Tainan City estimated for an M_w 7.2 scenario earthquake on the Chishan active fault. (Color online only)

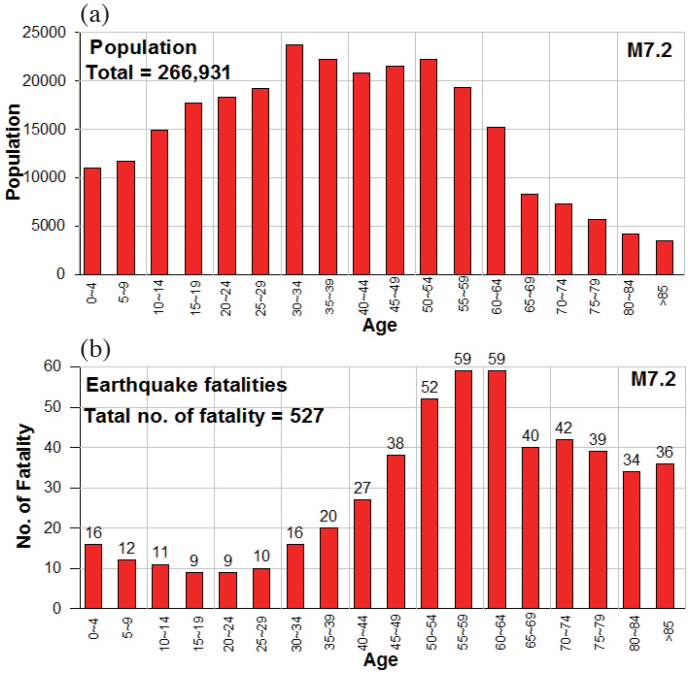

Fig. 18. Population (a) and the number of fatalities (b) in Pingtung County estimated for an M_w 7.2 scenario earthquake on the Chishan active fault. (Color online only)

Table 4. The number of fatality for different age groups in southern Taiwan estimated for M_w 7.2, 7.0, and 6.8 scenario earthquakes on the Chishan active fault.

Kaohsiung City																			
Age	**0 - 4**	**5 - 9**	**10 - 14**	**15 - 19**	**20 - 24**	**25 - 29**	**30 - 34**	**35 - 39**	**40 - 44**	**45 - 49**	**50 - 54**	**55 - 59**	**60 - 64**	**65 - 69**	**70 - 74**	**75 - 79**	**80 - 84**	**> 85**	**Total**
M_w 7.2	139	104	93	85	79	85	137	201	259	359	478	588	660	494	457	395	310	306	5230
M_w 7.0	114	86	76	69	64	69	111	164	212	294	390	479	541	406	375	325	255	255	4285
M_w 6.8	75	57	50	45	41	44	71	105	140	195	256	310	345	259	241	212	169	171	2786
Tainan City																			
Age	**0 - 4**	**5 - 9**	**10 - 14**	**15 - 19**	**20 - 24**	**25 - 29**	**30 - 34**	**35 - 39**	**40 - 44**	**45 - 49**	**50 - 54**	**55 - 59**	**60 - 64**	**65 - 69**	**70 - 74**	**75 - 79**	**80 - 84**	**> 85**	**Total**
M_w 7.2	71	53	48	43	40	45	71	93	122	176	242	276	280	196	215	208	177	156	2513
M_w 7.0	25	19	16	15	14	15	25	32	42	60	82	92	91	62	65	61	53	47	815
M_w 6.8	15	12	11	9	9	10	15	20	27	38	52	58	58	39	41	38	33	29	514
Pingtung County																			
Age	**0 - 4**	**5 - 9**	**10 - 14**	**15 - 19**	**20 - 24**	**25 - 29**	**30 - 34**	**35 - 39**	**40 - 44**	**45 - 49**	**50 - 54**	**55 - 59**	**60 - 64**	**65 - 69**	**70 - 74**	**75 - 79**	**80 - 84**	**> 85**	**Total**
M_w 7.2	16	12	11	9	9	10	16	20	27	38	52	59	59	40	42	39	34	36	527
M_w 7.0	3	2	2	2	2	2	3	4	5	9	12	14	15	11	13	13	10	7	130
M_w 6.8	0	0	0	0	0	0	0	0	0	0	0	0	1	0	1	1	0	0	3

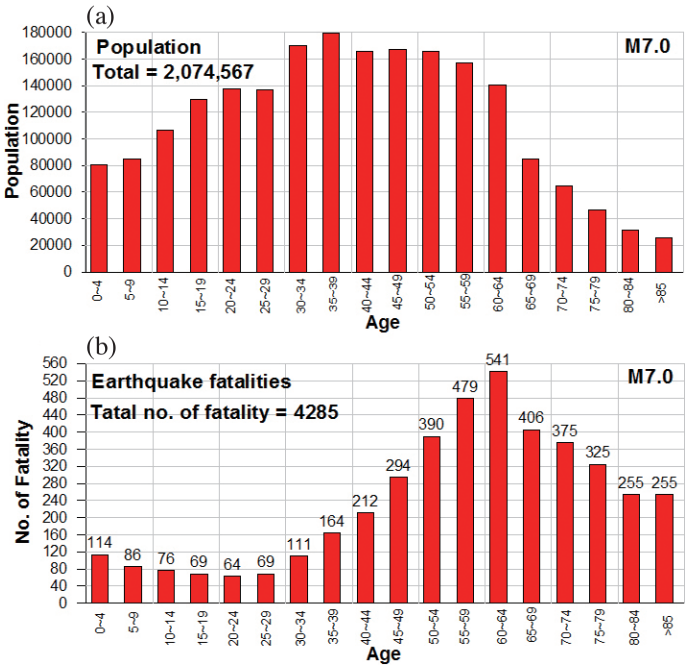

Fig. 19. Population (a) and the number of fatalities (b) in Kaohsiung City estimated for an M_w 7.0 scenario earthquake on the Chishan active fault. (Color online only)

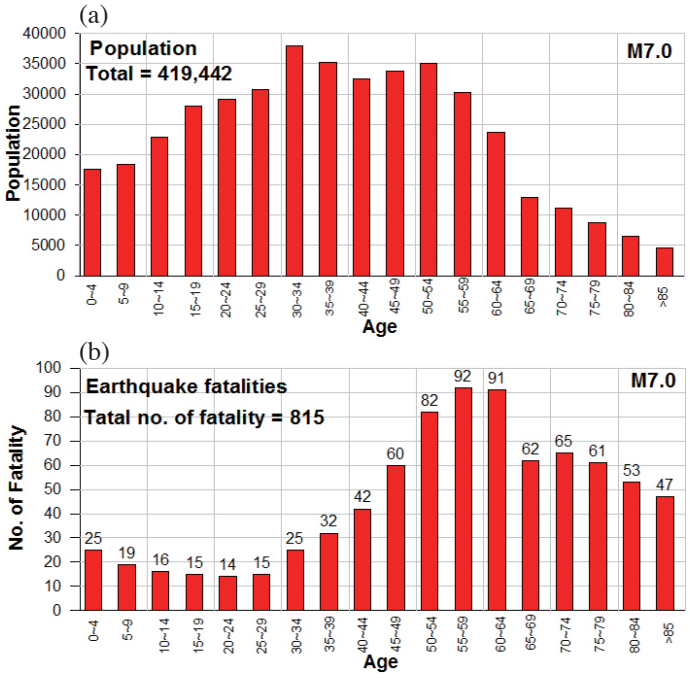

Fig. 20. Population (a) and the number of fatalities (b) in Tainan City estimated for an M_w 7.0 scenario earthquake on the Chishan active fault. (Color online only)

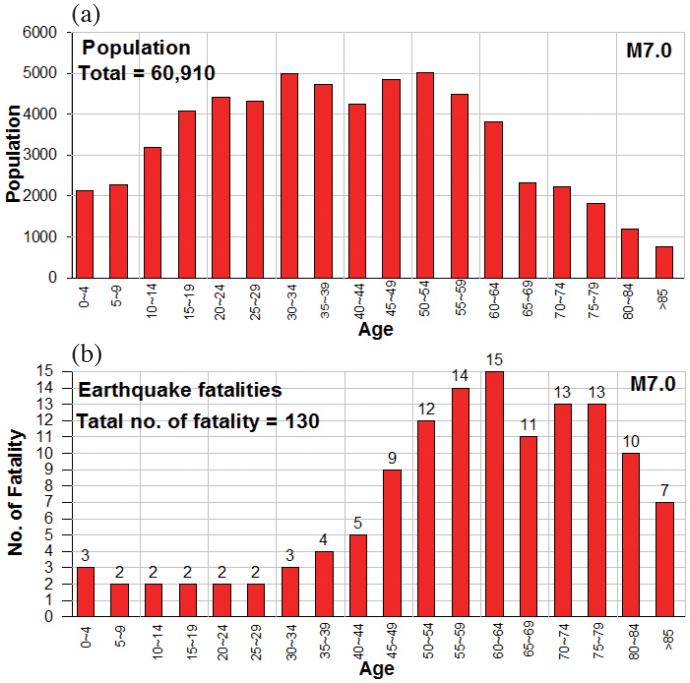

Fig. 21. Population (a) and the number of fatalities (b) in Pingtung County estimated for an M_w 7.0 scenario earthquake on the Chishan active fault. (Color online only)

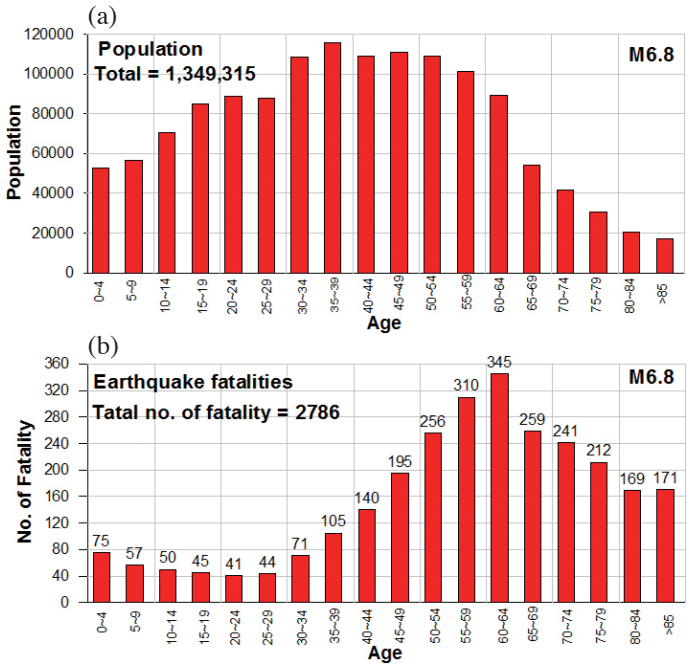

Fig. 22. Population (a) and the number of fatalities (b) in Kaohsiung City estimated for an M_w 6.8 scenario earthquake on the Chishan active fault. (Color online only)

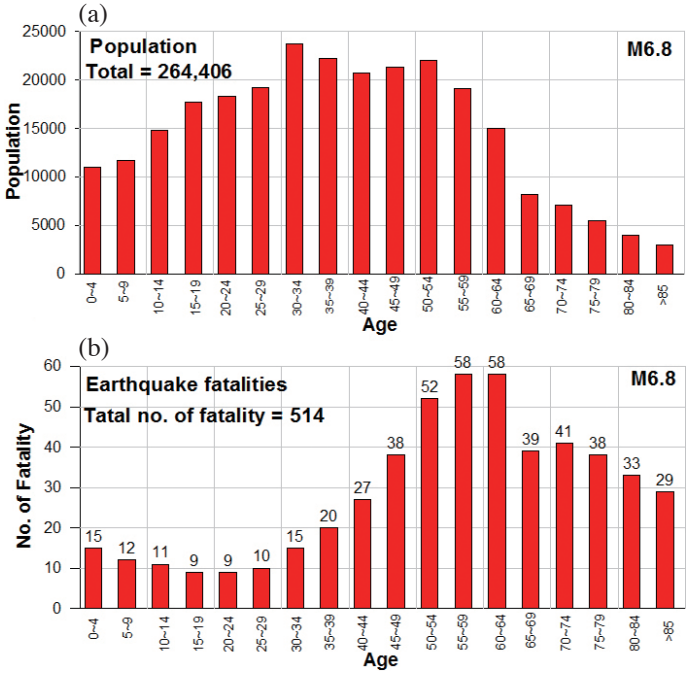

Fig. 23. Population (a) and the number of fatalities (b) in Tainan City estimated for an M_w 6.8 scenario earthquake on the Chishan active fault. (Color online only)

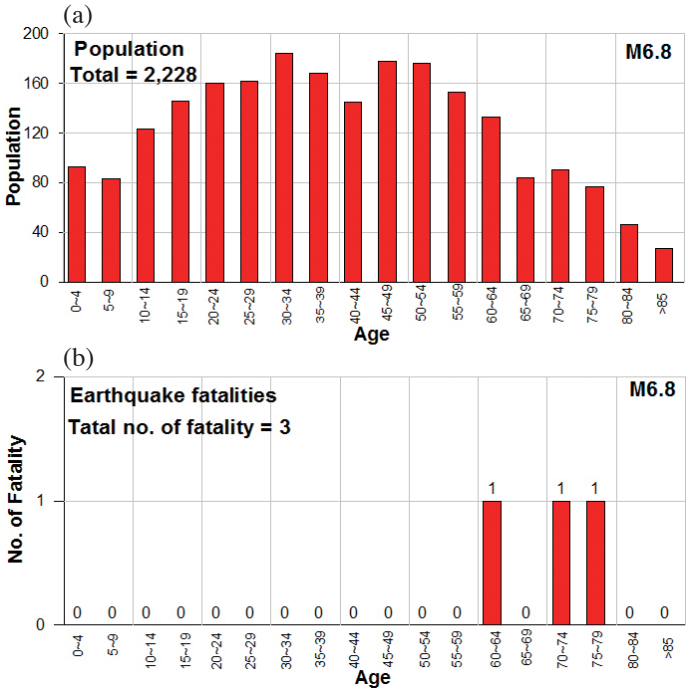

Fig. 24. Population (a) and the number of fatalities (b) in Pingtung County estimated for an M_w 6.8 scenario earthquake on the Chishan active fault. (Color online only)

for total populations of 2074567, 419442, and 60910, respectively in towns with estimated seismic intensity PGA greater than 250 gals of Kaohsiung City, Tainan City and Pingtung County, as shown in Fig. 10. The top panels in Figs. 22 - 24 show the age distributions for total populations of 1349315, 264406, and 2228, respectively in towns with estimated seismic intensity PGA greater than 250 gals of Kaohsiung City, Tainan City and Pingtung County, as shown in Fig. 13. The figures indicate that the population numbers start to decrease steadily above age 55.

The bottom panels in Figs. 19 - 21 show the age distributions for 4285, 815, and 130 fatalities, respectively, in Kaohsiung City, Tainan City and Pingtung County for M_w 7.0. Note that the numbers of fatalities stayed flat at an average of 84, 18, and 2, respectively, for people in Kaohsiung City, Tainan City and Pingtung County below age 35. For Kaohsiung City, as shown in Fig. 19b, the fatalities increase rapidly for those above age 45 and reach a high peak of 541 in the 60 - 64 age groups. The number of fatalities then drops rapidly back to 255 for those above age 85. For Tainan City, as shown in Fig. 20b, the numbers of fatalities increase rapidly for those above age 45 and reach a high peak of 92 in the 55 - 59 age groups. The number of fatalities then drops rapidly back to 47 for those above age 85. For Pingtung County, as shown in Fig. 21b, the numbers of fatalities increase rapidly for those above age 45 and reach a high peak of 15 in the 60 - 64 age groups. The number of fatalities then drops rapidly back to 7 for those above age 85.

The bottom panels in Figs. 22 - 24 show the age distributions for 2786, 514, and 3 fatalities, respectively in Kaohsiung City, Tainan City and Pingtung County for M_w 6.8. Note that the numbers of fatalities stayed flat at an average of 55, 12, and 0, respectively for people in Kaohsiung City, Tainan City, and Pingtung County below age 35. For Kaohsiung City, as shown in Fig. 22b, note that the fatalities increase rapidly for those above age 45 and reach a high peak of 345 in the 60 - 64 age groups. The number of fatalities then drops rapidly back to 171 for those above age 85. For Tainan City, as shown in Fig. 23b, note that the numbers of fatalities increase rapidly for those above age 45 and reach a high peak of 58 in the 55 - 64 age groups. The number of fatalities then drops rapidly back to 29 for those above age 85. For Pingtung County, as shown in Fig. 24b, note that the numbers of fatalities stay flat at about 0 for people below age 59.

The fatality rate is represented in this study as a function of age, i.e., higher fatality rate is expected for children and elders. However, this function is not consistent with the 2016 Meinong earthquake case. The average age of the fatalities in this event is 31, which is lower than the average for the population in Taiwan (http://www.new7.com.tw/NewsView.aspx?i =TXT20160217152652KCG). The fatality rate age dependence can be represented reasonably well according to the fact that the largest numbers of collapsed buildings and all large fatalities took place in the towns experiencing seismic intensity greater than 250 gal from the Chi-Chi earthquake (Tsai et al. 2001). The 6 February 2016 M_L 6.6 (M_w 6.3) Meinong earthquake caused 117 deaths.

The collapse of the Weiguan Building in Yongkang district resulted in the loss of 115 lives (Sun et al. 2016). From the seismic stations TAI1, the closest to this building at 4.4 km away, peak accelerations were recorded of 105 and 148 gals, in the NS and EW directions, respectively. Hence, the main cause was not the intense ground shaking, importantly, several structural features likely contributed to the building collapse. These irregular features include an irregular floor plan and elevation and poor (non-ductile) detailing practices. Standing more than 50-m tall, the building's first floor height vertical irregularity of 5.5 m compared to the uniform floor height of the remainder of the building (3.2 m), was more than 1.5 times greater. Non-ductile detailing practices included the use of short 90-degree hooks (rather than 135 degree hooks), insufficient beam-column confinement, and the use of inadequate coupler splices at column rebar (particularly notable in the first floor columns (Sun et al. 2016). Accordingly, the methodology implemented in this study was not suitable for a special case such as the inadequate structural building features in the Meinong earthquake.

In summary, the earthquake scenarios using M_w 7.2, 7.0, 6.8, on the Chishan fault estimated potential human casualties. As a result, the fatalities estimated in Kaohsiung City were 5230, 4285, and 2786, respectively for M_w 7.2, 7.0, and 6.8 higher than those for Tainan City and Pingtung County. The main reason is the high population density above 10000 persons per km^2, as shown in Fig. 2, present in Fongshan, Zuoying, Sanmin, Cianjin, Sinsing, Yancheng, Lingya Districts and between 5000 and 10000 persons per km^2 present in Nanzih and Gushan Districts in Kaohsiung City. The total population of these districts with estimated seismic intensity PGA greater than 250 gals reached 1013136 (National Statistics 2014).

The Ministry of Science and Technology (MOST) recently issued a warning that the probability for a magnitude 6.5 earthquake occurring in south Taiwan could be as high as 64% in the next 30 years (Wang et al. 2016). The study by Pai et al. (2007) showed the primary cause of death for victims of the Chi-Chi earthquake was structural failure. The building type was cited as one of the most important factors in fatalities. The human-fatality rates were found to be less in masonry and RC buildings as opposed mud-brick. The main cause lies in the difference in the capacity of different building types to resist strong shaking. In spite of building code revisions after 1999, better building quality is expected and the corresponding fatality rate should be reduced. There is great concern about the capacity of old buildings to resist strong shaking, especially for the more than 540 thousand households whose residences are over 50 years old. This number includes bungalows and 2 - 3 story houses in Kaohsiung City. Many of them are still in use. Even more worry some is that in Kaohsiung many of these old structures are used for shops in the city center where the population is highly concentrated. In an earthquake the consequences would be unthinkable. When a strong earthquake strikes, these old houses are vulnerable to collapse. In light of the MOST warning and the results of our study, we urge both the municipal and central governments to take effective seismic hazard mitigation measures in the highly urbanized areas with large numbers of old buildings in southern Taiwan.

5. CONCLUSIONS

According to above results and discussion, our findings are summarized as follows:

(1) From the maximum PGA Shake Map for an M_w 7.2 scenario earthquake on the Chishan active fault in southern Taiwan, areas with high PGA above 400 gals are located in the northeastern, central, and northern parts of southwestern Kaohsiung as well as the southern part of central Tainan. In addition, the area l patterns of high PGV above 50 cm s^{-1} are similar to that of PGA. The pattern of high MMI above VIII is similar to the contour pattern of PGV above 31 cm s^{-1}. In summary, the Shape Maps shown in Figs. 7 - 15 can provide a valuable database for site evaluation of critical facilities and land planning in regions with relatively high potential earthquake hazards in southern Taiwan.

(2) The cities located at similar distances from the Chishan fault, Tainan has relatively greater PGA and PGV than those in Kaohsiung City and Pingtung County were compared. This is due mainly to large site response factors in Tainan. For example, the site response amplification values of 2.89 and 2.97 for PGA and PGV, respectively, can be found in Madou from Figs. 3 and 4. High site response amplification values ranging from 1.0 - 2.7 for both PGA and PGV are present in western Tainan. On the other hand, seismic hazard in terms of PGA and PGV, shown in Figs. 7 and 8 in the vicinity of the Chishan fault, are not entirely dominated by the fault. The main reason is that the areas located in the vicinity of the Chishan fault are relative to the low site response factors, as shown in Figs. 3 and 4. Low site response amplification values [exp(r)] can be found ranging from 0.55 - 1.1 and 0.67 - 1.22 for PGA and PGV, respectively, are presented near the Chishan fault areas.

(3) Furthermore, the maximum ground motions and potential human fatalities were estimated by assuming three scenario earthquakes on the Chishan active fault in southern Taiwan. Note that the higher the magnitude for a scenario earthquake on the Chishan fault, the greater land coverage and population in areas with PGA above 250 gals, corresponding to CWB intensity VI. For example, the population in areas in Kaohsiung City with PGA above 250 gals from M_w 7.2, 7.0, 6.8, respectively are 2543359, 2074567, and 1349315. Moreover, the numbers of fatalities tend to increase rapidly for people

above age 45. The fatalities reached a high peak in age groups of 55 - 64 from these scenario earthquakes on the Chishan fault.

(4) Finally, the estimated fatalities in Kaohsiung City at 5230, 4285, and 2786, respectively, for M_w 7.2, 7.0, and 6.8 are higher than those estimated for Tainan City and Pingtung County. The main reason is the high population density above 10000 persons per km^2 present in Fongshan, Zuoying, Sanmin, Cianjin, Sinsing, Yancheng, Lingya Districts and between 5000 and 10000 persons per km^2 present in Nanzih and Gushan Districts in Kaohsiung City. Kaohsiung City has more than 540 thousands households whose residences are over 50 years old, including bungalows and 2 - 3 story houses. Many of them are still in use. Even more worrisome is that in Kaohsiung many of these old structures are used for shops in the city center where the population is highly concentrated. In an earthquake the consequences would be unthinkable. When a strong earthquake strikes, these old houses are vulnerable to collapse. In light of the MOST warning and the results of our study, I urge both the municipal and central governments to take effective seismic hazard mitigation measures in the highly urbanized areas with large numbers of old buildings in southern Taiwan.

Acknowledgements I thank the Central Weather Bureau of Taiwan for providing the strong motion data. I also appreciate greatly Yi-Ben Tsai, Chung-Han Chan, Ruey-Juin Rau, and the Two Anonymous Reviewers for their valuable comments, which improved the article. This research was supported by the Taiwan Earthquake Research Center (TEC) funded through Ministry of Science and Technology (MOST) with grant number MOST105-2116-M-244-001. The TEC contribution number for this article is 00130.

REFERENCES

Bolt, B. A. and N. A. Abrahamson, 2003: Estimation of strong seismic ground motion. In: Lee, W. H. K., H. Kanamori, P. C. Jennings, and C. Kisslinger (Eds.), International Handbook of Earthquake and Engineering Seismology, Part B, Academic Press, 983-1001.

Campbell, K. W. and Y. Bozorgnia, 2007: Campbell-Bozorgnia NGA ground motion relations for the geometric mean horizontal component of peak and spectral ground motion parameters. PEER Reports, PEER 2007/02, Pacific Earthquake Engineering Research Center, Berkeley, CA, USA.

CGS (Central Geological Survey), 2014: Active fault of Taiwan, Retrieved Mar. 15, 2014. Available at http://fault.moeacgs.gov.tw/MgFault/Home/pageMap?LFun=3.

Chen, C. C., C. T. Huang, R. H. Cherng, and V. Jeng, 2000: Preliminary investigation of damage to near fault buildings of the 1999 Chi-Chi Earthquake. *Earthquake Engineering and Engineering Seismology*, **2**, 79-92.

Coburn, A. and R. Spence, 1992: Earthquake Protection, John Wiley & Sons, Chichester, U.K., 355 pp.

Construction and Planning Agency, Ministry of the Interior, 2006: Performance-based Design Guideline and Commentary for Buildings. Taipei: Construction Magazine.

Council of agriculture, Executive Yuan, 2011: The 100 annual "Southern regional spatial planning of land resources". Retrieved Dec. 12, 2014. Available at http://211.22.161.202:81/ch/wp-content/uploads/2011Report/Chiayi_County/02_ch02.pdf.

Ho, C. S., 1982: Tectonic evolution of Taiwan, explanatory text of the tectonic map of Taiwan. Central Geologic Survey, The Ministry of economic Affairs, Taiwan, R.O.C.

Liu, K. S. and Y. B. Tsai, 2005: Attenuation relationships of peak ground acceleration and velocity for crustal earthquakes in Taiwan. *Bull. Seismol. Soc. Am.*, **95**, 1045-1058, doi: 10.1785/0120040162. [Link]

Liu, K. S. and Y. B. Tsai, 2014: Microzonation of seismic hazard potential in Tainan area. *J. Architect.,* **89**, 153-176, doi: 10.3966/101632122014090089009. [Link]

Liu, K. S. and Y. B. Tsai, 2015a: A refined Vs30 map for Taiwan based on attenuation relationships of ground motion. *Terr. Atmos. Ocean. Sci.*, **26**, 631-653, doi: 10.3319/TAO.2015.05.11.01(TC). [Link]

Liu, K. S. and Y. B. Tsai, 2015b: Microzonation of seismic hazard potential in Chiayi area. *J. Chin. Inst. Civ. Hydraul. Eng.*, **27**, 309-321.

Liu, K. S. and Y. B. Tsai, 2016a: Microzonation of seismic hazards and assessment of potential human fatality in Chianan Area, Taiwan. *Bull. Seismol. Soc. Am.*, **106**, 141-157, doi: 10.1785/0120150182. [Link]

Liu, K. S. and Y. B. Tsai, 2016b: Microzonation of seismic hazard potential in Kaohsiung Area. *J. Architect.*, **96**, 153-176, doi: 10.3966/101632122016060096006. [Link]

Liu, K. S., T. C. Shin, and Y. B. Tsai, 1999: A free field strong motion network in Taiwan: TSMIP. *Terr. Atmos. Ocean. Sci.*, **10**, 377-396, doi: 10.3319/TAO.1999.10.2.377(T). [Link]

Liu, K. S., Y. B. Tsai, and B. S. Lin, 2013a: A study on fault type and site effect (Vs30) parameters in the attenuation relationships of peak ground acceleration and velocity in Ilan, Taiwan. *Bull. Seismol. Soc. Am.*, **103**, 1823-1845, doi: 10.1785/0120120065. [Link]

Liu, K. S., Y. B. Tsai, and K. P. Chen, 2013b: Estimation of seismic hazard potential in Taiwan based on shake maps. *Nat. Hazards*, **69**, 2233-2262, doi: 10.1007/s11069-013-0804-x. [Link]

Liu, K. S., Y. B. Tsai, C. H. Chang, and B. S. Lin, 2014: A study of site effects in Ilan, Taiwan based on attenuation relationships of spectral acceleration. *Bull. Seismol.*

Soc. Am., **104**, 2467-2490, doi: 10.1785/0120130238. [Link]

National Statistics, Republic of China (Taiwan), 2014: Age structure of the resident population by township/city/district. Retrieved Apr. 21, 2014. Available at https://eng.stat.gov.tw/mp.asp?mp=5.

Pai, C. H., Y. M. Tien, and T. L. Teng, 2007: A study of the human-fatality rate in near-fault regions using the Victim Attribute Database. *Nat. Hazards*, **42**, 19-35, doi: 10.1007/s11069-006-9043-8. [Link]

Shyu, J. B. H., K. Sieh, Y. G. Chen, and C. S. Liu, 2005: Neotectonic architecture of Taiwan and its implications for future large earthquakes. *J. Geophys. Res.*, **110**, B08402, doi: 10.1029/2004JB003251. [Link]

Shyu, J. B. H., Y. R. Chuang, Y. L. Chen, Y. R. Lee, and C. T. Cheng, 2016: A new on-land seismogenic structure source database from the Taiwan Earthquake Model (TEM) project for seismic hazard analysis of Taiwan. *Terr. Atmos. Ocean. Sci.*, **27**, 311-323, doi: 10.3319/TAO.2015.11.27.02(TEM). [Link]

Sun, J., T. Hutchinson, K. Clahan, F. Menq, E. Lo, W. J. Chang, C. C. Tsai, and K. F. Ma, 2016: Geotechnical reconnaissance of the 2016 Mw6.3 Meinong Earthquake, Taiwan. GEER Reconnaissance Report, GEER-046, Geotechnical Extreme Events Reconnaissance Association, doi: 10.18118/G6PK5J. [Link]

Tsai, Y. B., T. M. Yu, H. L. Chao, and C. P. Lee, 2001: Spatial distribution and age dependence of human-fatality rates from the Chi-Chi, Taiwan, Earthquake of 21 September 1999. *Bull. Seismol. Soc. Am.*, **91**, 1298-1309, doi: 10.1785/0120000740. [Link]

Wald, D. J., V. Quitoriano, T. Heaton, and H. Kanamori, 1999: Relationships between peak ground acceleration, peak ground velocity and Modified Mercalli Intensity in California. *Earthq. Spectra*, **15**, 557-564, doi: 10.1193/1.1586058. [Link]

Wang, Y. J., C. H. Chan, Y. T. Lee, K. F. Ma, J. B. H. Shyu, R. J. Rau, and C. T. Cheng, 2016: Probabilistic seismic hazard assessment for Taiwan. *Terr. Atmos. Ocean. Sci.*, **27**, 325-340, doi: 10.3319/TAO.2016.05.03.01(TEM). [Link]

Wells, D. L. and K. J. Coppersmith, 1994: New empirical relationships among magnitude, rupture length, rupture width, rupture area, and surface displacement. *Bull. Seismol. Soc. Am.*, **84**, 974-1002.

Yeh, C. H., C. H. Loh, and K. C. Tsai, 2006: Overview of Taiwan earthquake loss estimation system. *Nat. Hazards*, **37**, 23-37, doi: 10.1007/s11069-005-4654-z. [Link]

Yu, T. M., 2004: The Relations of earthquake disasters with respect to surface fault rupture, crustal movement, and strong ground motion: Using two central taiwan earthquakes in 1935 and 1999 as examples. Ph.D. Thesis, National Central University, Chungli, Taiwan, 209 pp. (in Chinese)